

## Resistivity Imaging for Geothermal Exploration, using Controlled-Source EM where Magneto-Telluric is not Applicable: Model and Field Study.

Jean-François Girard<sup>1</sup>, Nicolas Coppo<sup>1</sup>, Pierre Wawrzyniak<sup>1</sup>, Bernard Bourgeois<sup>1</sup>, Jean-Michel Baltassat<sup>1</sup>, Alain Gadalia<sup>1</sup>

<sup>1</sup>Bureau de Recherches Géologiques et Minières, 3 av. Claude Guillemin, BP 36009, 45060 Orléans Cedex 2, France.

jf.girard@brgm.fr, n.coppo@brgm.fr, p.wawrzyniak@brgm.fr, b.bourgeois@brgm.fr, jm.baltassat@brgm.fr, a.gadalia@brgm.fr

**Keywords:** CSEM, Resistivity Imaging, Borehole Casing, Martinique, Geothermal Exploration

### ABSTRACT

Resistivity imaging is a key parameter in most geothermal exploration programs, and particularly in volcanic environment. It is assumed that resistivity variations allow imaging the caprock, but also hydrothermal weathering or preferential water flow. The geothermal fluid is generally brine water which drastically decreases the electrical resistivity and the temperature increase also decreases resistivity. The resistivity signatures for several conceptual geothermal reservoirs can be found in the literature.

Magneto-telluric (MT) is generally used to image resistivity variations down-to a relevant investigation depth of several kilometers. Based on natural source signal, MT prospection efficiency depends on the Sun activity during the survey but moreover depends on the noise conditions. In many cases, because industrial activities have been developed close to the geothermal resource, the noise conditions make it difficult to obtain reliable MT tensors and hence a good resistivity image. Generally, the only way to counter is recording longer time series, to apply robust noise filtering and combining with a remote filtering. The noise issue in MT prospection is even more drastic in Island context.

We investigated the substitution of controlled-source EM instead of MT measurements close to urbanized area. The distance constraints to respect the far field conditions are so challenging that they are often logically not possible. Indeed, when it is possible to measure the receiver stations far enough from the source, the distortion due to the controlled-source disappear. But when the conditions for applying standard processing of CSAMT are not fulfilled, it is necessary to consider the source effect to interpret properly the EM response.

We have studied and performed EM imaging in the near field, using a pair of pre-existing boreholes to inject high current into the ground through metallic casings. Based on numerical modeling, we propose a methodology to obtain maps and section of apparent resistivity. The results obtained were confronted to previous geophysical campaign results performed in the 1980's and recent shallow prospection. This measuring protocol was applied to prospect the Lamentin area (Martinique, Lesser Antilles, France). This survey was performed in 2013 within the framework of a large exploration program founded by the FEDER, ADEME, Regional Council and SMEM designed to explore the geothermal potential of Martinique.

### 1. INTRODUCTION

Resistivity imaging is a key parameter in most geothermal exploration programs, and particularly in volcanic environment. It is assumed that resistivity variations allow imaging the caprock, but also hydrothermal weathering or preferential water flow. The geothermal fluid is generally brine water which drastically decreases the electrical resistivity and the temperature increase also decreases resistivity. One can find a snapshot in the use of geophysics in the “Geothermal Exploration Best Practices – Geology, Exploration Drilling, Geochemistry, Geophysics”, published by the IGA Academy (2013). Based on a European initiative, in the framework of the I-Get European project, a review has been published (Baltassat et al., 2009).

Several organizations, and dedicated workshops have proposed to hierarchize the needs to improve the exploration methods, and one could quote the “Roadmap for strategic development of geothermal exploration technologies” after the 38th workshop on geothermal reservoir engineering in Stanford (Philips et al., 2013). Resistivity imaging has been particularly used in geothermal exploration, because of the strong link of the electrical resistivity with fluid content, weathering signature, large depth of investigation and logically easier than seismic for large depth. Progress in EM prospection have benefited from the seabed logging (or marine CSEM) which quickly developed since 2000 (Edwards, 2005), at least in terms of imagery, and management of large dataset (Commer and Newman, 2009) and combined use with dense seismic and borehole data. A recent review of EM use in geothermal exploration has been done by Munoz (2014). He gives a list of progress, many field applications all over the world. He underlines successes but also failures in rare documented case studies. Major success rely on the strong correlation of the resistivity with the key geothermal parameters, but equivalent solutions, lack of knowledge of the local geological signature may lead to severe errors.

In the first part of this paper, we present the basic principle of CSEM and the specific way we applied it. Indeed, we injected electrical current using the metallic casing of boreholes to enhance the EM response. We explain the data processing and illustrate the performance of the array with a numerical synthetic example.

The second part of this paper deals with a field application. The geothermal potential of Martinique Island (Lesser Antilles, France) has been extensively investigated since more than 50 years. The first exploration started in the 60' in the Plaine du Lamentin (south of Fort-de-France) and has been extended in this area in the 80's and orientated towards the southeastern flank of the Montagne Pelée. Then, the southwestern flank of the Montagne Pelée and the Anses d'Arlet were identified of potential interest and explored in the 2000's. Finally, three exploration wells were drilled in the Plaine du Lamentin in 2001 and confirmed the presence of a

medium temperature geothermal resource. In 2013, resistivity imaging was chosen to map this later area, in order to estimate the extent of the reservoir. Combined with the borehole geological logs, a new geological and geochemical survey, other available geophysical results (gravity, magnetic, shallow resistivity) the goal was to get a better evaluation of the geothermal resource of the Lamentin area.

This campaign provided useful results for the geothermal exploration but thanks to a previous deep DC electrical resistivity campaign in the 80's along a profile crossing the area, it has been possible to validate the proposed the methodology at depth. An airborne TEM survey performed over all Martinique in 2013 allowed validating shallow CSEM results. In the second part of the paper, we compare the apparent resistivity maps and sections with the TEM and deep ERT.

## 2. CONTROLLED SOURCE ELECTROMAGNETISM

The Controlled Source Electro-Magnetism (CSEM) is a geophysical method based on the imagery of electrical resistivity. Unlike MT method, the signal source is not passive but generated by a transmitter. The first interest is that it is less sensitive to man-made electromagnetic noise due to powerlines, electrical plants, etc...which make EM passive methods such as MT difficult or almost impossible in noisy area. The duration for 6 to 8 frequencies, starting from 0.125 Hz to 1 kHz, is generally 1 hour. Depending on site conditions (current intensity, noise) these parameters should be adapted to obtain sufficient signal to noise ratio as in Figure 1.

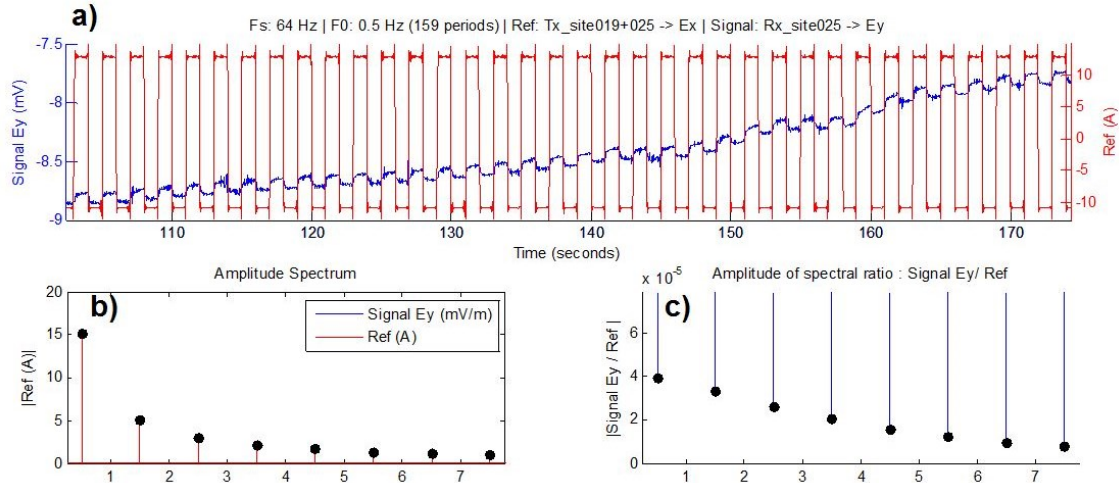


**Figure 1: Example of CSEM data processing for an electric channel: a) time serieof injected current (~7 A) and recorded signal for a 200 m length dipole, b) frequency spectrum for Current c) modulus of ratio E/I. Black dots indicate data at measuring frequencies (here : 0.5 Hz, 1.5 Hz, etc...)**

If the controlled source is far enough, several kilometers from the survey area for frequencies  $> 1$  Hz, the far field approximation is fulfilled and the CSEM data can be processed as audio MT data (controlled source audio magneto-telluric) corresponding to the shallowest response of MT. Considering a targeted investigation depth of 2000 m or more, the far field assumption cannot be reached sometimes and especially in islands. Then, the controlled-source EM data should be processed with another protocol than in MT.

The depth of investigation is controlled both by the signal frequency and by geometry of the transmitter. Particularly, if instead of using surface current injection, metallic casing of boreholes are used to enhance de contact resistance but also inject current closer to the targeted depth (see Figure 2). In this latter case, the geometry of the well and the length of the metallic casing should be considered to estimate the source effect and remove it.

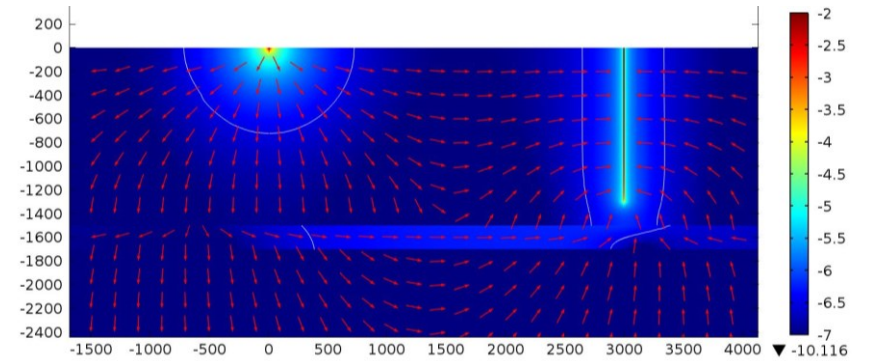


**Figure 2: Electrical current density (log scale, A/m<sup>2</sup>) below a surface injection (left) and when using a metallic casing (right side, down to 1300 m here) for 2 Hz current injection. The current flows preferably at depth all along the borehole and particularly in the conductive layer. The ratio target response versus primary source is more favorable with the casing injection.**

Using borehole metallic casing as a long electrode was already used, and for instance one could refer to Hatanaka et al. (2005) for a recent use for geothermal energy, but this advantages of this array was discussed by Bourgeois and Girard (2010) for monitoring CO<sub>2</sub> injection in a limestone deep aquifer.

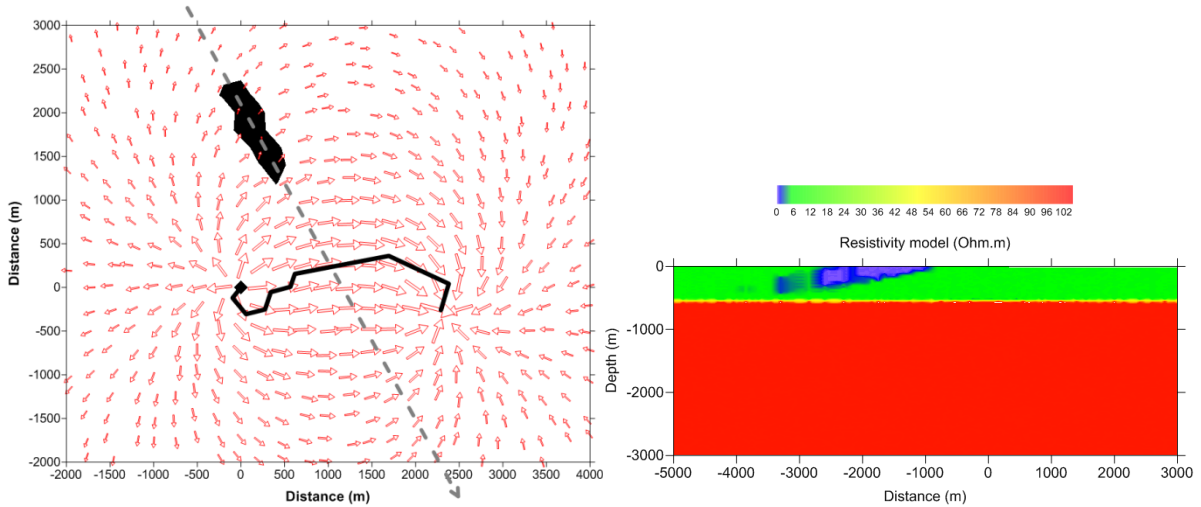


**Figure 3: In-phase Electric field (8 Hz) measured at surface, in black the cable between two boreholes and to the north, the extension of a conductive anomaly. Right, a resistivity cross-section: ground is 5 Ohm.m down to 700 m then 100 Ohm.m deeper. A targeted tilted conductive anomaly (0.3 Ohm.m) is displayed.**

Nowadays, we provide the results as apparent resistivity map and sections (corrected from frequency and geometrical factors, topic discussed in this paper). Note that, if it is possible to derive geometrical information from a single MT sounding (strike direction, dipping, etc...), a single CSEM station should be considered as a deep electrical sounding and do not provide geometrical information by it-self. When used along profiles or with a homogeneous density over a surface, the resistivity maps and sections provide geometrical information.

Because the resistivity is estimated from the electric field components, it is not necessary to measure magnetic field at stations for CSEM use only. That makes the logistic easier and thanks to shorter recording duration, several CSEM soundings could be performed the same day with the same equipment.

For the sake of demonstration, we simulate the electric field measured at surface of a 2 layers ground (5 Ohm.m then 100 Ohm.m deeper) with a conductive anomaly in the vicinity. We consider a current injection via a pair of boreholes 2.5 km apart and connected by a cable (see Figure 3). This scenario is directly suggested by the field experiment discussed in the next part.

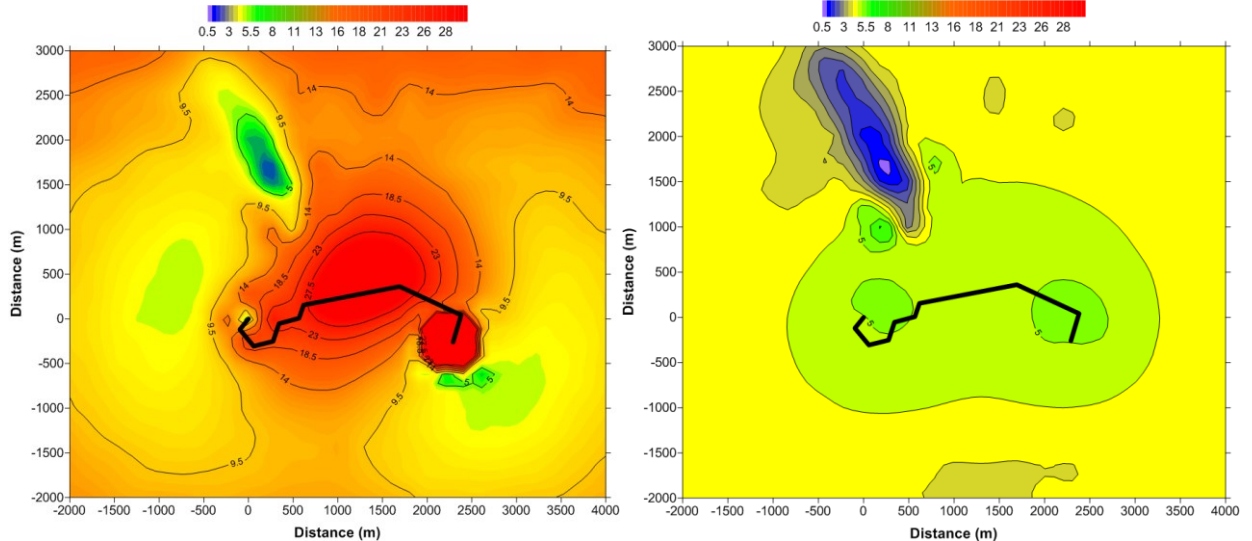


**Figure 4: Left, 8 Hz in-phase electric field amplitude converted in a highly distorted apparent resistivity map (in Ohm.m) using a pure geometric factor (DC assumption). Right after a normalization based on the computation of the EM field at 8 Hz over a homogeneous medium at 5 Ohm.m, the anomaly is well resolved with few artifacts.**

As in DC electrical imaging, one can convert the in-phase electric field in apparent resistivity considering the transmitter point injection and the location of the receivers. This well-known transformation is straightforward and classically used to normalized

data before inversion and electrical resistivity tomography (ERT). This is the classical way of using arrays like rectangle or gradient, popular in mining exploration: the resistivity map highlight the anomalies below the area covered by receivers. As depicted in Figure 4, this approach is not suitable for measurements over a several kilometers area, in a 5 Ohm.m environment at 8 Hz. Numerous artifacts appears with a high dynamic range, larger than the anomaly in a homogeneous ground. If one considers the use of normalizing the measured field by the synthetic response at 8 Hz, over a homogeneous medium with 5 ohm.m.resistivity, one gets a far better resistivity image (Figure 4, right). It is important to compute the frequency dependent normalizing field above a ground resistivity with value close to the field to take into account phase rotation:

$$\rho_{\text{apparent}} = \frac{E_{\text{in-phase}}^{\text{measured}}(f)}{E_{\text{in-phase}}^{\text{calculated at } \rho=\text{cste}}(f)} * \rho(\text{cste}) = \frac{E_{\text{in-phase}}^{\text{measured}}(8 \text{ Hz})}{E_{\text{in-phase}}^{\rho=5}(8 \text{ Hz})} * 5$$

This normalization aims to attenuate 2 effects: a geometrical effect (due to the proper transmitter geometry) and a frequency effect link with the phase rotation and attenuation in the ground. Figure 5 shows a comparison of these two terms.

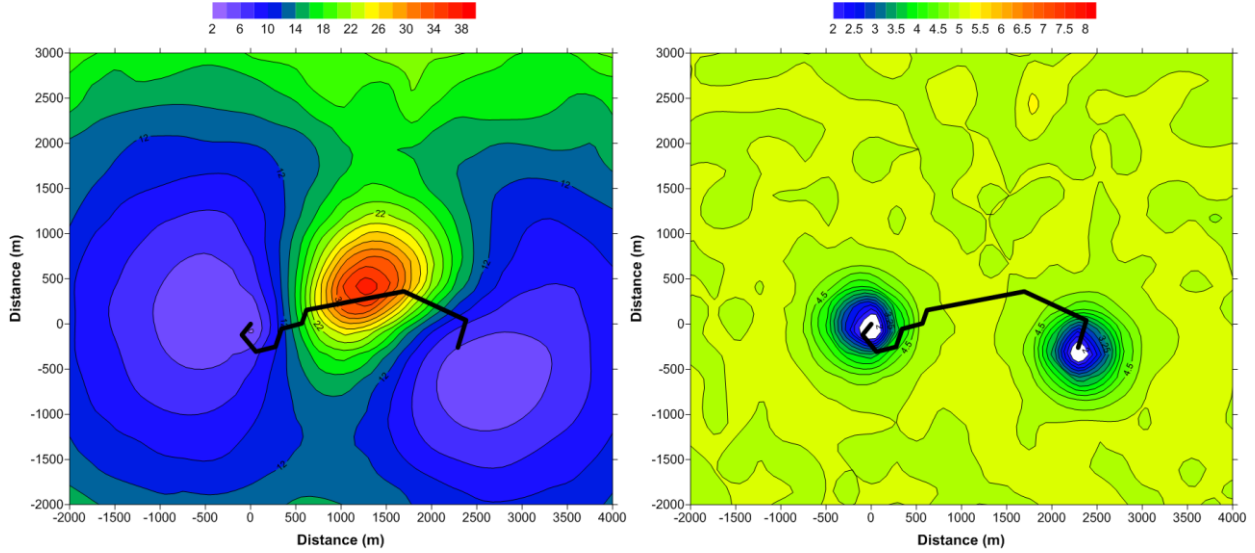


**Figure 5:** 8 Hz in-phase electric field converted in apparent resistivity map (no anomaly here, only homogeneous medium at 5 Ohm.m). Left, error introduced when normalizing with the exact geometry but with a DC assumption at 5 Ohm.m. Right, error introduced when normalizing by surface electrode response (instead of 450 m long boreholes) calculated at 8 Hz over a 5 Ohm.m ground.

The interesting fact is that in a quite conductive environment (5 Ohm.m here) and considering frequencies  $> 2$  Hz, the exact borehole equipment and the uncertainty in the resistance contact all along the casing are of secondary importance in comparison with the frequency effect which creates phase rotation and attenuation of the electric field. The stronger effect being computable, this is the approach we have used in the field survey keeping in mind the limitation of the apparent resistivity approach, as illustrated below in Figure 6.

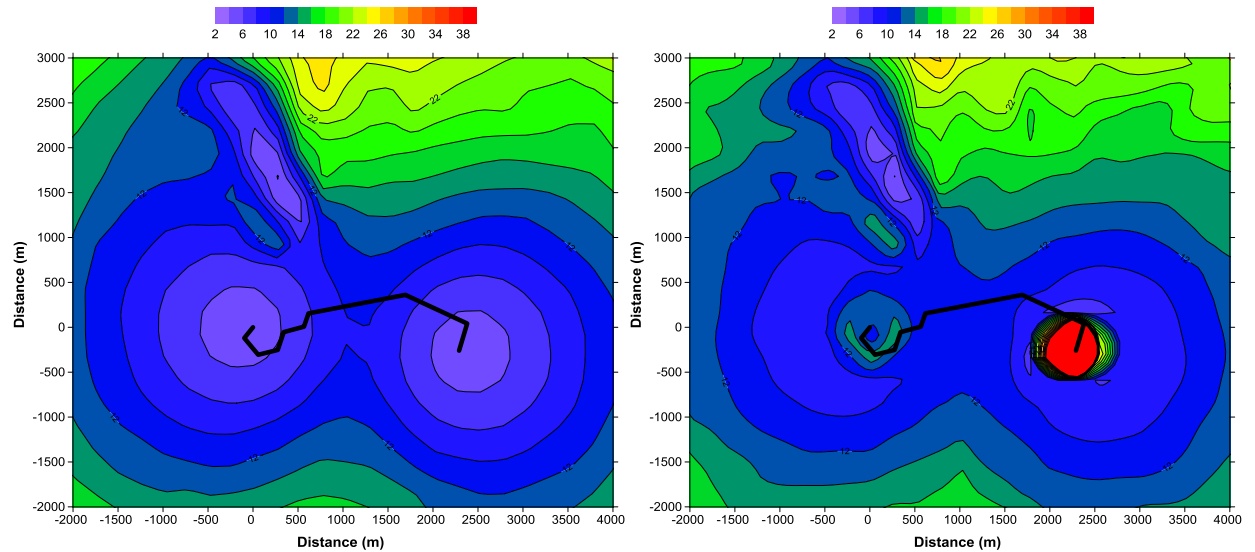


**Figure 6:** 0.1 Hz in-phase electric field converted in apparent resistivity map (anomaly + 2 layers ground): DC assumption geometric factor correction and the normalization using frequency computation provide almost the same result.

At 0.1 Hz, the skin depth is more than 3500 m and the response of the conductive bodies (2 metallic boreholes + northern anomaly located in the first 400m) merge and dominate the EM response. Despite the resistivity below 700 m is homogeneous equal to 100 Ohm.m, the apparent resistivity is not at all a direct image of the ground. When the distance between the boreholes (or point injections) are similar or greater than skin depth, the “source” effect cannot be suppressed so easily and a full inversion is needed to overcome this difficulty. This is a current topic of development in our team and is out of the scope of this paper. Nevertheless, the suitable depth and frequency range was in agreement with the needs for the survey in the Lamentin area.

### 3. CSEM FIELD SURVEY IN THE LAMENTIN AREA

The Lamentin area is partly urbanized (including housing and commercial centers close to Fort-de-France) and is equipped with an international airport. The remaining zone is whether densely cultivated whether in the mangrove. Considering the high anthropic noise (powerlines and various installations) it was then proposed to investigate at depth using a Controlled-Source Electro-Magnetism approach (CSEM).

The conditions for applying standard processing of CSAMT being not fulfilled, it was necessary to compute a specific normalization to correct the source effect. Indeed, when it is possible to measure the receiver stations far enough from the source, the distortion due to the controlled-source disappear. But the geography of the area of interest and the pre-existing exploration boreholes used to inject current at depth make it impossible in this case.

#### 3.1 EXPLORATION RESULTS

45 receiver stations were measured over a 10x10 km area during 6 days. 35 stations were measured on-shore, with electric dipoles and magnetic coils. 10 stations were measured off-shore, in shallow water (1 to 5 meters depth) in the Lamentin bay. The frequency band was covered using 7 fundamental frequencies ranging from 0.125 up to 512 Hz with a factor 4 between two adjacent frequencies. The signal waveform was a square wave generating many harmonics allowing to double records. GPS positioning and time synchronization was used. Resistivity maps at single frequency were converted using the normalization described before. An estimation of the investigation depth is based on the skin depth ( $\delta$ ):

$$\text{Investigation depth} = \frac{503}{\sqrt{2}} * \sqrt{\frac{\rho(\Omega m)}{f(Hz)}}$$

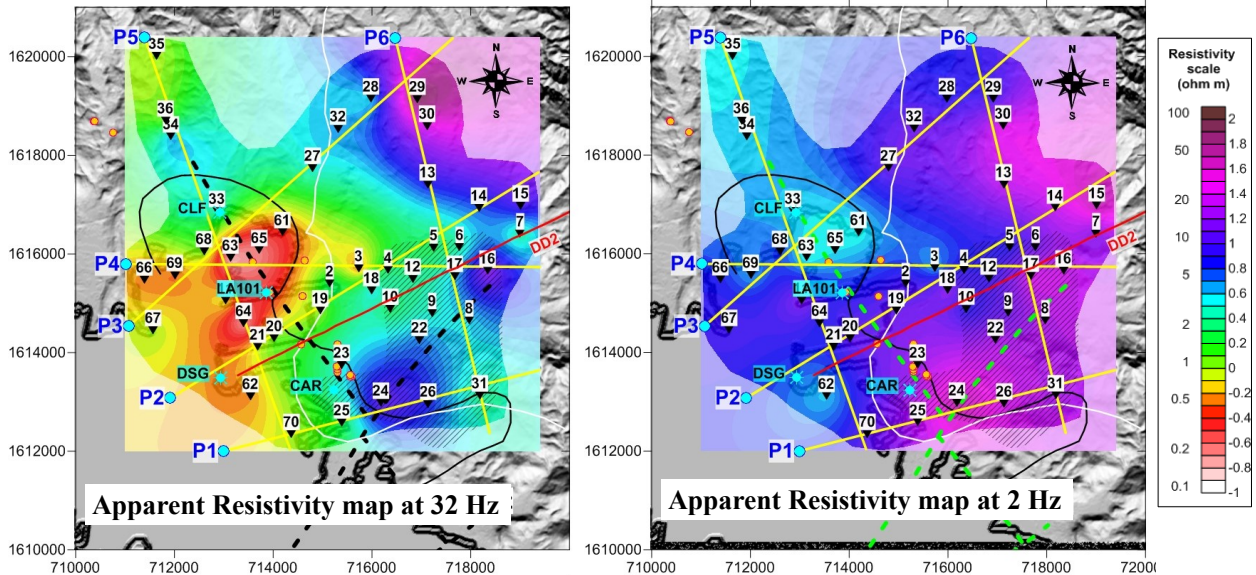


**Figure 7:** Left, apparent resistivity map (CSEM 2013), from the in-phase Electric field component, TX Frequency 32 Hz, ( $\delta/\sqrt{2} = 141$  m) and right TX frequency 2 Hz ( $\delta/\sqrt{2} = 562$  m), both normalization by MAMx2-400m, 5  $\Omega.m$ , at corresponding frequency.

For frequencies higher than 4 Hz, the general pattern is quite similar (see Figure 7, left). It reveals a very conductive anomaly ( $< 3$  Ohm.m in apparent resistivity) centered on the borehole LA101. This anomaly is clearly limited laterally and migrate in the NW direction with decreasing frequency. The general shape of this conductive zone is de-correlated from the coast line and the off-shore stations do not appear as outliers. The sea water intrusion being important in all the western part of the covered area, this continuity is in agreement with the known hydrogeological context.

A drastic change appears for frequencies equal or lower than 2 Hz (see Figure 7, right). Apparent resistivity appear then higher, contrasts are smoother and the boundary of the basement with less sea water intrusion is well correlated with existing boreholes and the few older geophysical surveys results. A less resistive trend appear going N/N-W but only 4 stations (33,34,35,36) along a straight profile was measured in this zone and it is not possible yet to speak about a channeling of deep brine coming from the northern topography associated to the volcanic system of the Carbets.

Despite all the limitations, we extracted several profiles, using the frequency along the Y-axis, and we depict in Figure 8 the apparent resistivity pseudo-section along a profile crossing the 4 boreholes drilled in the early 2000. On the north-western side, a

shallow resistive zone correspond well with the topographic end of the Carbet (no topographic is applied here, but it flatten the top of the conductive zone. At the abscisse 3000 m, a clear change in resistivity pattern is well correlated with a major fault (Westercamp et al., 1990). When one overlay the isotherms curves derive from temperature logs, it follows closely the conductive anomaly which is also well correlated with the kaolinite dominating clay considered as the more permeable medium (Mas et al., 2003) and location of geothermal fluid up-flow corresponding with known geothermal spring traces in surface. On the south/south-east side, the abrupt change is well correlated with the dry wells Carrere and Desgras (this later, a bit apart from the profile P5) and absence of surface springs indications.

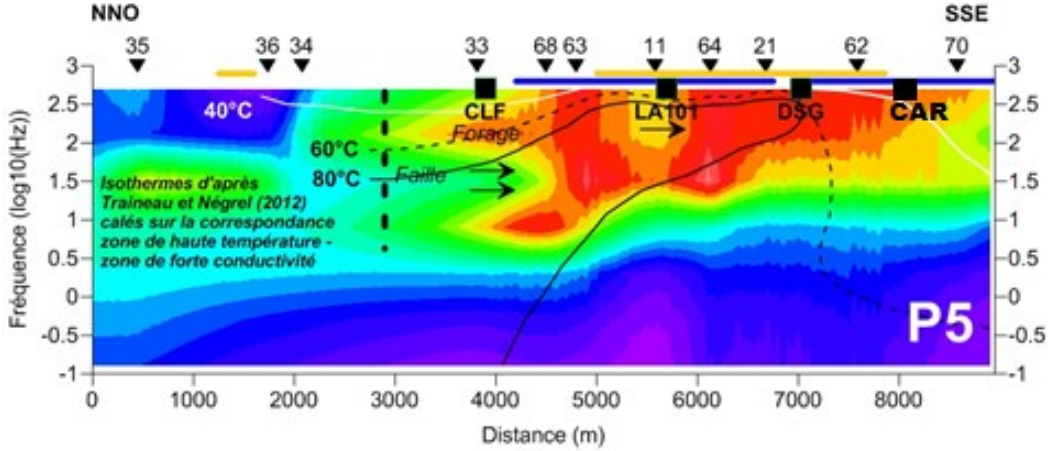


**Figure 8:** On P5 are surimposed isotherms, from Trainneau et Négrel (2012). Boreholes locations are indicated by black squares CLF= Californie, DSG=Pointes-Desgras, CAR=Carrère. Horizontal arrows below CLF indicate the main water flow, Trainneau et Négrel (2012). The black vertical dashed line are resistivity discontinuities coincident with 2 known faults.

The Lamentin plain has known at least two periods of geothermal activity and the classical conceptual model of a reservoir rich in illite covered by a caprock rich in smectite. The issue involving petrology, geology and water geochemistry in this complicated context is out of the scope of this article, but it is striking that the deepening of the isotherm between absciss 4000-5000m, which do not rely on any in-situ temperature measurement is, at first look, not compatible with the geophysical result. It would suggest a lateral arrival of the geothermal fluid more probable than a vertical root. To enlarge the CSEM measurement westward (and Fort-de-France, the island largest city) was not considered during this short survey (10 days in total) but given the coherent results obtain when mixing on-shore and off-shore measurements, and the signal to noise ratio obtained with the used of the boreholes Carrere and Desgras as current injectors up to 8 km away, it would suggest to densify the measurement in the north and north-west part of the area.

### 3.2 CSEM RESULTS VALIDATED

The Lamentin plain has a rich exploration history, started in the 1980's, for geothermal resource but also on hydrological point of view. Especially, an airborne survey using skyTEM system over all Martinique Island has been performed in 2013, coordinated by BRGM, the French geological survey. It is straightforward to compare high frequency CSEM response with TEM mapping.

Figure 9 shows the good correlation between apparent resistivity at 128 Hz (investigation depth~70m) and the resistivity layer at 60m. The white line delineate the CSEM area, based on the interpolation of 45 stations. The black dashed line delineate the resistivity mapping using airborne TEM. One should keep in mind that investigation depth is limited to 200 m maximum in this low resistive environment, and the dense housing prevent from using helicopter in may places. Moreover, powerlines drastically deteriorate TEM response, particularly at depth. It is a good combination to fill the holes in the TEM map with CSEM results, and a constant factor 3 was applied to surimpose TEM and CSEM results in Figure 9. The correlation is very good, even if the distance between CSEM stations is around 400 m compared to airborn TEM 10m along flight lines (100m or 200m generally in between, except in area studied for hydrology with denser data).

Another comparison, at depth, was possible with the results of DC electrical imaging performed in 1984 (Puviland and Doré). Data sheets were copied and inverted in 2D along the profile named DD2 on the maps. A dipole-dipole profile, using MN spacing 500m was performed before the airport was built. The comparison if depicted in Figure 10. A constant factor of nearly 10 is observed (gross estimation) but eh general pattern is in good agreement.

Thanks to these 2 comparisons, it was demonstrated that in such an environment, CSEM resistivity imaging can be applied successfully and provide useful insight for geothermal resource exploration.

### 4. CONCLUSIONS

A variant of on-shore CSEM method application using boreholes is presented. The processing is demonstrated first on numerical example then compared in the field to independent results (deep ERT and shallow TEM). It proved to be logically interesting and efficient to map resistivity in such anthropic area for geothermal exploration.

Known limitation in the use of apparent resistivity is recalled and limits were calculated in the studied environment. Nevertheless, the way to overcome it is clear: 3D CSEM inversion. It is currently developed in our team and this case study will be especially interesting to apply it thanks to the a priori knowledge and local validation that exists from previous surveys and boreholes.

Bridge between clay mineralogy and electrical resistivity is also a subject of research currently under investigation.

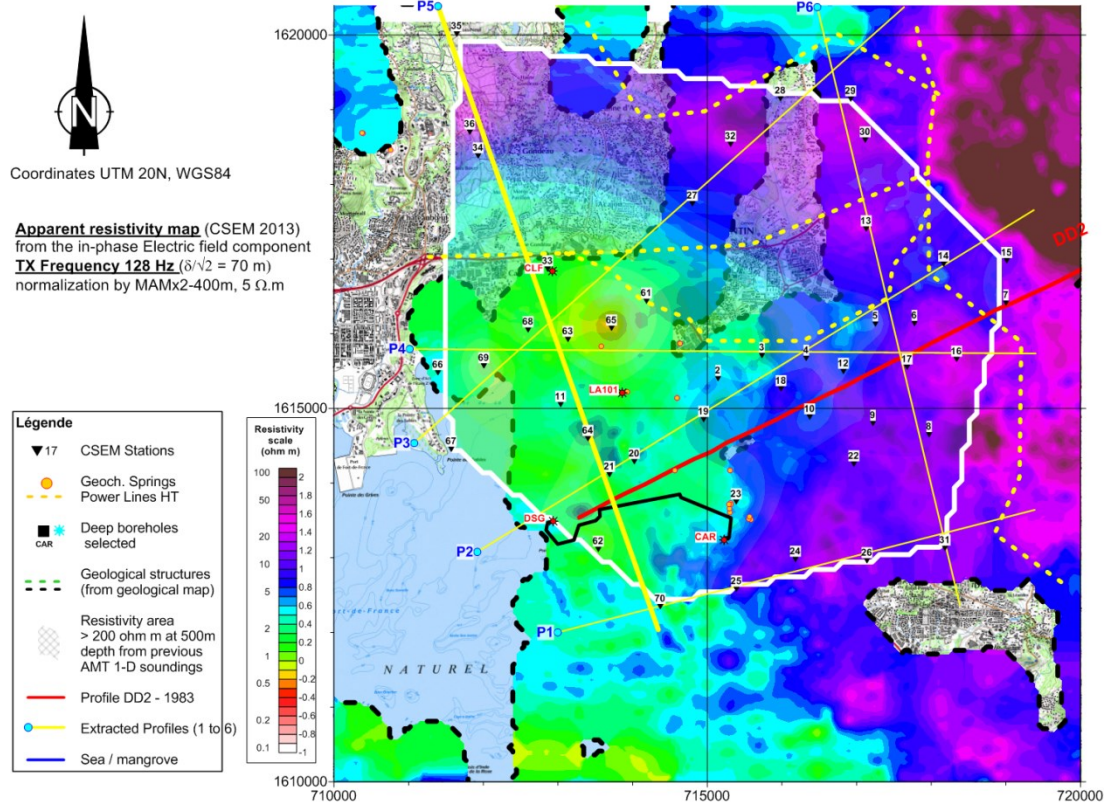


**Figure 9: Apparent resistivity map (csem 2013 – 128 Hz ~ 70 m) jointly presented with Airborne TEM – 60m – (MarTEM survey, 2013)**

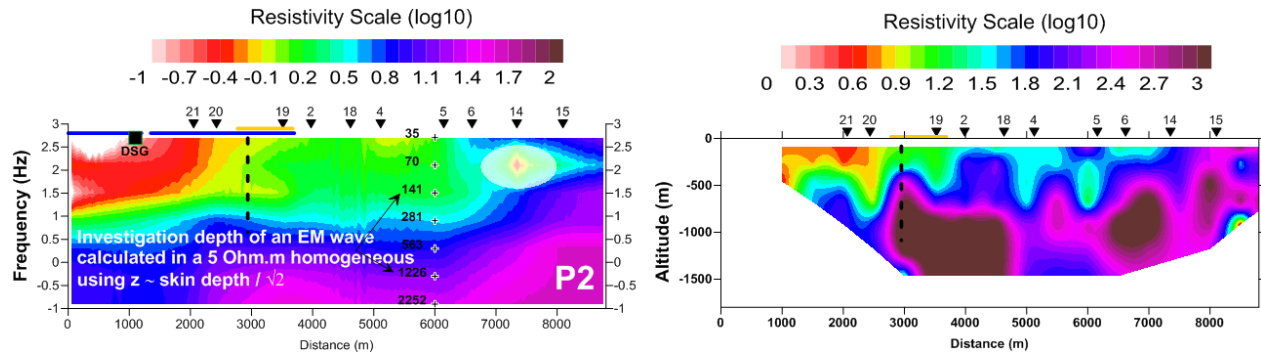


**Figure 10: Left, Dipole-Dipole profile n°2 reprocessed (Puvilland et Doré, 1984) in log10 of inverted (2D) resistivity, and pseudo-sections of apparent resistivity from CSEM data for profiles P2 (partly along DD profile n°2).**

## ACKNOWLEDGEMENTS

The authors wish to thank the FEDER and ADEME institutions, the Conseil Régional and the Syndicat Mixte d'Electricité de la Martinique (SMEM) for funding this project. The numerical modeling of CSEM synthetic case was performed in the framework of the Integrated Methods for Advanced Geothermal Exploration - IMAGE project, which has received funding from the European Union's Seventh Programme for research, technological development and demonstration under grant agreement No: 608553.

## REFERENCES

Baltassat J.M., Bertani R., Bruhn D., Ciuffi S., Fabriol H., Fiordelisi A., Giolito C., Holl H.G., Karytsas C., Kepinska B., Manzella A., Mazotti A., Mendrinos D., Moeck I., Perticone I., Pussak M., Thorwart K., Wolfgramm M., 2009, Integrated Geophysical exploration technologies for deep fractured geothermal systems (I-GET) – Review of geophysical exploration methods applied to deep fractured geothermal reservoir. Final report, BRGM/RP-57089-FR, European Research Program FP6-2004-Energy-3.

Bourgeois B, Girard J-F. First modelling results of the EM response of a CO<sub>2</sub> storage in the Paris basin. *Oil & Gas Science and Technology - Rev. IFP* 2010; 65(4): 597-614

Commer M. and Newman G. A. (2009) - Three-dimensional controlled-source electromagnetic and magnetotelluric joint inversion, *Geophys. J. Int.* 178, 1305–1316.

Edwards N. (2005) - Marine Controlled Source Electromagnetic: principles, methodologies, future commercial applications, *Surveys in Geophysics*, 26:675–700.

Gadalía, A., J.M. Baltassat, V. Bouchot, S. Carigt, N. Coppo, F. Gal, J.F. Girard, A. Gutierrez, T. Jacob, G. Martelet, S. Rad, A.L. Tailame, H. Trainea, B. Vittecoq, P. Wawrzyniak, C. Zammit : Compléments d'exploration géothermique en Martinique : conclusions et recommandations pour les zones de la Montagne Pelée, des Anses d'Arlet, des Pitons du Carbet et du Lamentin, (2014), Rapport final BRGM/RP-FR, 227 p, 75 fig., 7 tabl., 4 ann., 1 CD.

Hatanaka H., Tetsuo A., Mizunaga H., Ushijima K. (2005) Threedimensional modelling and inversion of the Mise-à-la-Masse data using a steel-casing borehole, *Proceedings of the World Geothermal Congress*, Antalya, 24-29 April 2005.

Mas A., Patrier A., Beaufort D., Genter A., 2003, Clay-mineral signatures of fossil and active hydrothermal circulations in the geothermal system of the Lamentin Plain, Martinique, *Journal of Volcanology and Geothermal Research*, 124, pp. 195-218.

Munoz G., 2014, Exploring for Geothermal Resources with Electromagnetic Methods, *Surv Geophys* (2014) 35:101–122, DOI 10.1007/s10712-013-9236-0

Philips B. R., Ziegos J., Thorsteinsson H., Hass E., A ROADMAP FOR STRATEGIC DEVELOPMENT OF GEOTHERMAL EXPLORATION TECHNOLOGIES, 2013, *Proceedings of 38th Workshop on Geothermal Reservoir Engineering*, Stanford University, Stanford, California, February 11-13, 2013.

Trainea H., Bouchot V., Carigt S., Gadalía A.: Compléments d'exploration géothermique en Martinique : volet géologie, Rapport intermédiaire, (2013), BRGM/RP-62349-FR, 153 p., 69 fig., 9 tabl., 3 ann.

Trainea H., Négrel G. (2012) – Evaluation préalable de la ressource géothermale du Lamentin, Martinique. Rapport intermédiaire. BRGM/RP-61759-FR, 79 p., 24 fig., 5 tabl., 1 ann..

Westercamp D, Pelletier B, Thibaut PM, Trainea H, Andreieff P (1990) Carte géologique de la France (1/50 000), feuille Martinique, BRGM, Orléans.